Effects of Thermal Ageing on the Wear Behavior of the Cerium Modified Al-18Si-3.6Cu Alloy

Krishnaraddi Gangal[1], Dayanand M. Goudar*[, 2], Julfikar Haider[3], Devendra K[4], Rajendrakumar V. Kadi[2]

[1] *Department of Mechanical Engineering, Rural Engineering College, Hulkoti, India-5822205*

[2] *Department of Mechanical Engineering, Tontadarya College of Engineering, Gadag, India-582101*

[3]*Department of Engineering, Manchester Metropolitan University, Chester Street, Manchester, M1 5GD, UK*

[4] *Smt. Kamala & Sri Venkappa M. Agadi College of Engineering& Technology, Lakshmeshwar-India-582116*

Corresponding author
Dayanand M.Goudar
Department of Mechanical Engineering,
Tontadarya College of Engineering, Gadag,
India-582101
Email: dmgoudartcel@gmail.com

Abstract: In the present investigation, Al-18Si-3.6Cu alloy was modified by Cerium (Ce) and heat treated (T6) and aged for 1, 3, 5, and 7 hrs at 210°C. The resulting microstructures revealed that the addition of Ce as a modifier changed the morphology of the primary Si from coarse with a sharp edge to spherical, large-acicular/needlelike eutectic Si into a fibrous state, and dendrite Al phase into round branches with less interface separation. After thermal aging, the microstructure of the modified alloy revealed no change in the morphology of the primary Si phase. However, a considerable change in the eutectic Si phase and the formation of fine precipitates of Al_2Cu and Al_2CeSi intermetallics in the matrix. Hardness was found to be significantly higher in the modified and age-hardened alloys. A Pin-on-Disc wear tester was used to investigate the dry sliding wear behavior of alloys at different loads (10, 20, 30, and 40 N) and 1.0 m/s sliding velocity. The results indicated that the wear rate in the modified alloy was lower than the base alloy. Furthermore, the modified alloy after 5hr age hardening demonstrated high wear resistance and improved wear bearing capacity compared to the 1, 3, and 7 hr age hardened alloys.

Keywords: Hypereutectic Al-Si-Cu alloy, Cerium modifier, Age hardening, Hardness, Wear, Coefficient of friction

1. Introduction

Aluminum silicon alloys have many industrial applications due to their high strength to weight ratios, good corrosion inhibition, good machinability and wear resistance [1]. Hypereutectic Al–Si alloys have low density, high specific stiffness, and high temperature resistance, wear resistance and, low coefficient of thermal expansion and therefore, are used to produce engine block without cylinder liner, and these properties are mostly attributed to the primary Si phase [2]. The Al-Si alloy with approximately 17-18 wt.% Si content shows the best fluidity and, consequently, the best castability. The form, size, and distribution of the primary Si and eutectic phases have a significant impact on the wear properties of the hypereutectic Al-Si alloy [3]. The hypereutectic Al-Si alloy consists of coarse plate/star-like primary Si and needle shape eutectic phases in the dendrite Al matrix. The wear rate at lower loads is less as the coarse primary Si particles serve as load-bearing components [2]. However, under high loading conditions, the coarse primary Si particles break and easily get separated away from the matrix. According to a study [4], the coarse grains are more prone to fracture, which raise the possibility of a third-body wear mechanism since the broken pieces of Si act as an abrasive media. Elmadagli et al. [5] investigated the effect of microstructure (Si wt%, particle size, and morphology) on the wear behavior of Al-Si alloys and reported that increasing the Si content enhanced the transition load, but had only minor effects on the wear rate. A decrease in the aspect ratio or size of the Si particles, on the other hand, increased both wear resistance and the transition load. The hypereutectic Al-Si alloy having 17 wt.% Si content showed better wear resistance [6]. The fine and spherical primary Si phase in the Al matrix was found to increase the wear resistance significantly [1]. Different techniques such as semi-solid processing, electromagnetic stirring, the rapid solidification process, twin roll casting, and ultrasonic vibration have been used successfully to refine microstructures.

Grain refiners (inoculants) introduced during solidification act as nucleation sites for the primary Si particles to promote heterogeneous nucleation [7]. Several rare earth elements have been added in Al-Si alloys to modify the morphology and microstructure of the eutectic Si phase [8-9]. Aluminum phosphate compound (AlP) is formed when phosphorus and aluminum react at high temperatures and this compound has a high melting point (2530ºC) and serves as a heterogeneous nucleation site for the primary Si and allows the formation of a larger number of

primary Si grains, yielding smaller individual grains [9]. Phosphor is most commonly added as red phosphorus, phosphate salt, or Cu-P master alloy. However, all of these have flaws, particularly the use of P in an Al melt, which brings Occupational Health and Safety (OHS) hazards that can stymie industrial adoption. When AlP comes into contact with moisture, it emits a poisonous and combustible phosphine gas [10]. Modifying elements such as calcium, sodium, strontium, and antimony are used to transform the eutectic Si phase's needle/acicular form into a fine fibrous/laminar form. The rare earth elements such as Yttrium (Y) and Cerium (Ce) have also been found to be effective modifiers, in general, which have a high tendency to alter the Si phase into a fibrous structure, improving its mechanical and wear properties [11]. Zhang et al. [12], reported that the addition of Ce element to Al-18Si alloy resulted in a spherical form of the primary Si and finer lamellar or fibrous eutectic network. However, there was little impact on the eutectic Si that was close to the primary Si particles. According to Li et al. [13], Ce addition to the Al-20Si alloy, resulted in an improvement in both ductility and tensile strength, due to a decrease in the size and change in the morphology of the primary and eutectic Si crystals. Ce addition refined the primary Si grains of an Al-17Si alloy and reduced the liquid temperature. Maja vončina et al. [14] reported that Ce modifies the eutectic Si structure and induces a transition from a coarse flake-like and acicular shape to a fine fibrous structure and discrete particles with an increasing concentration. The addition of Ce improved the tensile strength and ductility of the Al−Si alloys through modifying their microstructures. Gröbner et al. [15] reported that the Ce phases serve as the nucleation sites for the aluminum or silicon crystals in both the hypo and hypereutectic Al−Si alloys. However, Mehdi and Malakhov [16] found that the addition of 0.03wt%–0.2wt% Ce neither modified the microstructure nor noticeably affected the grain size of the Al–Si alloys. Ao et al. [17] investigated the effect Ce addition on the microstructures and mechanical properties of the A380 aluminum alloy. It was reported that the modification effect was no longer noticeable when the added Ce content was greater than 0.5wt% and the 0.3wt% Ce alloy depicted a high ultimate tensile strength and ductility.

The ternary Al-Si alloy is widely used in the automotive industry due to its increasing importance for bringing lightweight and high strength characteristics. The precipitation of the intermetallic phase and the solubility of ternary elements in the matrix are the two most crucial factors to take into account when choosing the ternary elements. Solid solubility strengthens existing phases while ensuring modification through changes in equilibrium rather than solute

buildup in the liquid [18]. The Al-Si-Cu alloy shows higher strength than binary Al-Si alloy and their corrosion resistance is better than Al-Cu alloys. The addition of Cu to the Al-Si alloy increases the wear resistance of the alloy by increasing the matrix solid solubility and the formation of hard and brittle intermetallic Al_2Cu phase [19]. According to Ceschini and Toschi [20], the addition of modest amounts of Si, Cu, and Mg causes the precipitation of Al_2Cu and Mg_2Si phases, which improves hardness and strength, and hence the wear resistance of Al alloys. Dasgupta and Bose [21] concluded that the wear resistance of the Al-Si alloy increased with Cu addition because of the Al_2Cu phase. Another study [22], showed that the wear rate is not appreciably affected by the addition of Cu. However, the addition of Cu increased the transition load. The influence of the combined action of grain refiner and modifier on dry sliding wear of the Al-12Si-3Cu alloy showed the best wear resistance at higher loads [23]. For a given Al−Si alloy, the Si particle shape can be modified by using modifiers during the melting and casting process and or heat treatment methods.

The impact of heat treatment for Al−Si base alloys containing Cu and/or Mg have been reported [24]. Traditional solutionzing and ageing processes are employed to alter the morphology of Si particles in Al-Si based alloys [25]. Hazra et al. [26] reported that the improvement in the wear resistance at the higher temperature after heat treatment was attributed to the additional strengthening from age hardening that occurred during the wear process. This improvement was attributed to microstructural modification upon heat treatment. The enhancement in the wear properties of Al-Si-Cu alloys after heat treatment has been mainly attributed to the formation of non-equilibrium Al_2Cu precipitates within the primary dendrites and changes in Si particle morphology. The amount and coarsening of precipitation vary depending on the ageing temperature and its duration. The addition of 0.05 wt. % Ce changed the morphology of the Al-Cu phase in an Al-Si cast alloy from crumbled to fully form [27]. In addition, Ce element reacts with Si to form $CeSi_2$ which may promote the heterogeneous nucleation of the intermetallic phase. However, excessive Ce will lead to the loss of Si content, which in turn reduces the fraction of the main strengthening phase. Therefore, adding suitable Ce content will be an effective method to modify the Al_2Cu phase in Al-Si-Cu alloys [28].

However, investigations are lacking on the wear behavior of thermally aged and Cerium modified hypereutectic Al-Si alloy. In the present work, the influence of ageing time on the wear

behavior of Ce modified (T6) and thermally aged Al-18Si-3Cu alloy was investigated and compared with the basic and modified alloys.

2. Experimentation

In the present work, an electrical resistance furnace was used to melt the base (Al-18Si-3.6Cu) alloy at 850°C (Make: NANOTECH, Chennai, India; Power 3-6 kW; Material loading capacity, 1-10 kg). The melt temperature was continuously monitored with K-type thermocouples. The base alloy of 3 kg was loaded into the preheated (500°C) crucible. The preheated Al–15wt% Ce master alloy pieces were added into the melt and were then stirred for 25 min to ensure composition homogeneity. To ensure a low hydrogen content, the melt was degassed with 6 g of solid hexachloroethane (C_2Cl_6). Billets were prepared by pouring the molten metal into a metal mold that had been preheated at 150ºC. The chemical composition of as-cast alloys was determined by X-ray fluorescence (XRF) using a Philips X-ray spectrometer (model PW 1480); the findings are presented in Table 1. A report [17] states that once the additional Ce concentration exceeded 0.5 wt%, the modification effect was no longer noticeable. Therefore, in this study, 0.34 wt.% of Cerium was added to the base alloy. For the microstructural study, the samples were ground, polished, and etched using a Keller etchant and examined through an optical (ZYNAX) microscope and a field emission scanning electron microscope (Model: JEOL JSM-6480LV) using secondary electron (SE) and Working Depth (WD) imaging modes, whereas chemical compositions of the constituent phases are examined using an energy dispersive X-ray (EDX) micro-analyzer attached to the SEM. The SEM is operated at an acceleration voltage of 10-30 kV. The base, modified and age-hardened alloys were machined into cylindrical pins of 30mm × Φ10 mm. The T6 heat treatment was carried out in a muffle furnace. The alloy was solution treated at a temperature of 500 °C for 1 h and quenched to room temperature followed by an aging treatment at 210 °C for 1hr, 3hr, 5hr and 7 hr.

Table 1. The chemical constitution of the Al-18Si-3.6Cu-0.34Ce alloy (Grade3XX.X)

Elements	Si	Cu	Ce	Al
Weight%	18	3.66	0.34	Balance

Brinell hardness (BH) test was conducted according to ASTM E10 using a 2.5 mm diameter ball indenter (SAROJ, Optical Brinell Hardness Tester, B-3000). Readings of the microhardness of the alloys were taken 20 times under a load of 62.5 kg. Wear tests of the unmodified, modified and modified heat-treated samples were carried out on a Pin-on-Disc wear testing machine [DUCOM WEAR & FRICTION MONITOR -TR-20LE) having a EN-32 steel disk. The loads were varied at 10, 20, 30, and 40 N while the sliding velocity and sliding distance were kept to 1.0 m/s and 2000 m respectively. Figure 1 shows the wear testing set-up used in this investigation.

Figure 1. Dry sliding Pin on Disc type wear testing machine

Volumetric wear rate and wear resistance were calculated by using equation (1) and equation (2)

$$V = \frac{\Delta m}{\rho} \tag{1}$$

$$\text{Wear resistance} = \rho/\Delta m \tag{2}$$

Where ρ is the density and Δm (weight of a pin before test - weight of a pin after test) is the sliding wear measured as the weight loss of the samples using a high precision digital weighing scale (WENSAR, PGB-301, 0.01 mg accuracy). Interface temperature measurement at the pin during the sliding was carried out using a chromel-alumel thermocouple placed at 1.5 mm away from the sliding surface. Interface temperature and friction force were recorded after every 2 min of sliding time and the average values were reported. The ratio of the average frictional force to the normal force is known as the average coefficient of friction.

3. Results and discussion

3.1. Microstructures

Figure 2(a) shows the optical microstructure of the base alloy, which consisted of a block like the polygonal form of primary Si with sharp edges, with random distribution of long acicular eutectic Si phase and the distinctive reticular-shape of inter metallic phases and columnar grains of α-Al matrix. The microstructure of the Al-18Si-3.4Cu-0.3Ce alloy (Figure 2b) shows reduced size, rounded and more regular Si edges and angles, increased α-Al spheroidization, and uneven distribution of the intermetallic phases at the interface between the eutectic Si and α-Al matrix. The addition of Ce clearly transformed the large-acicular, plate-like eutectic Si into a fibrous and dendrite Al phase into round branches with less interface separation. Figure 2(c-f) shows the microstructures of the modified and T6 heat treated alloys at different aging times. As observed, in the microstructure of 1hr and 3hr age-hardened alloys (Figure 2c,d) the spheroidization of both primary Si of eutectic silicon phases and precipitation of fine intermetallic phases were observed. The microstructure of the alloy after 5 hr of ageing revealed the formation and homogenous distribution of coherent fine Al_2Cu precipitates at the grain boundary as well as changes in the eutectic Si into fine and spherical particles. The microstructure of the modified and 7 hr age-hardened alloy is shown in Figure 2(f). It is observed that after the age-hardening process, there is no change in the shape of primary and eutectic Si. However, the coarse Al_2Cu phase with a branched network can be noticed in the 7 hr age-hardened alloy.

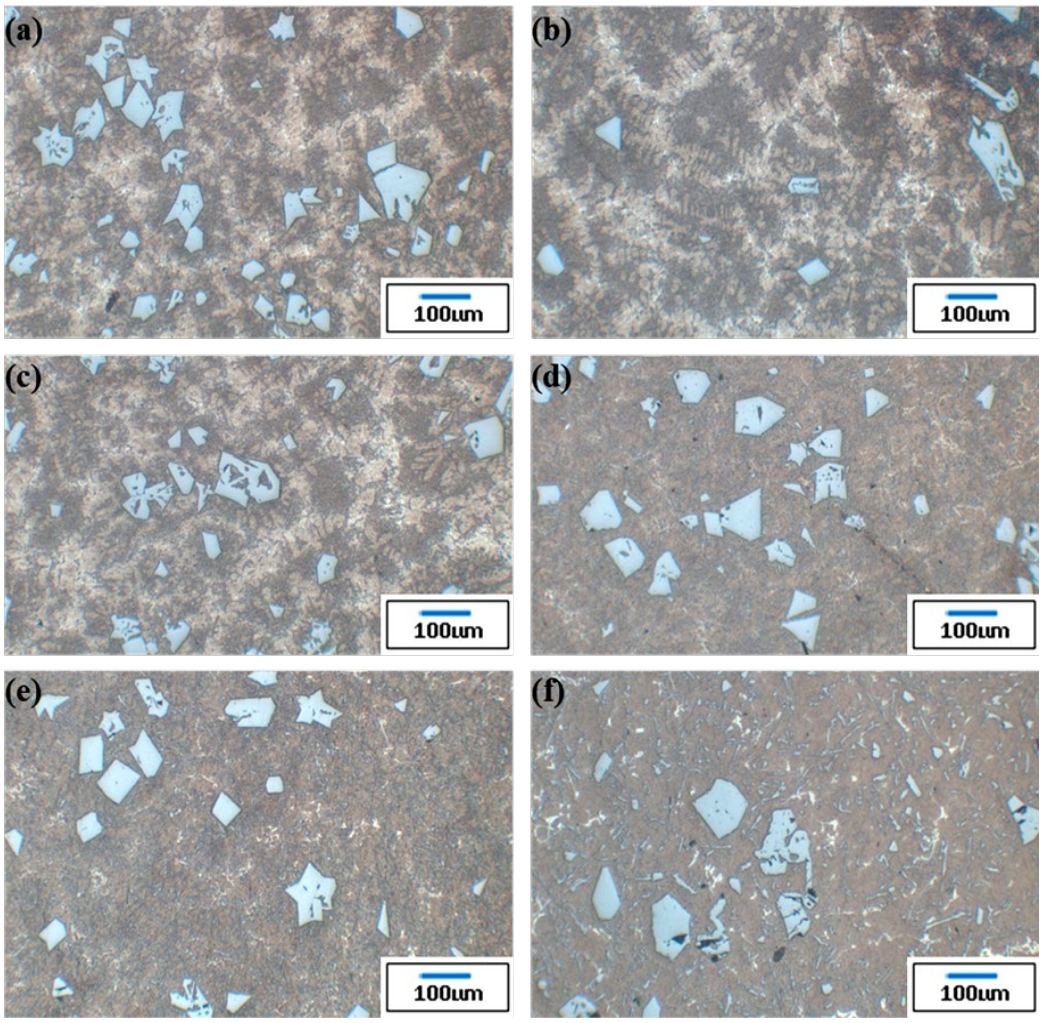

Figure 2. Optical microstructure of (a) base (b) modified (c) 1 hr age (d) 3 hr (e) 5 hr and (f) 7 hr age hardened alloy

SEM/EDS images of the base alloy (Figure 3) showed the presence of plate-like coarse primary Si (light gray), eutectic needles/plate, and θ (Al_2Cu) intermetallic compounds (white contrast) randomly scattered throughout the matrix. The EDS results of the phase composition of the cast alloy is shown Table 2. Figure 4 shows the SEM /EDS microstructure of the modified alloy. It was clearly observed that the addition of Ce significantly changed the morphology of the primary Si, the eutectic phase and α-Al grains. Improved alloys have the primary Si particles of spherical form corners, refined eutectic Si, and significantly modified with globular α-Al matrix. It was clear that the uneven distribution of θ and Cerium rich (AlCe and Al-Si-Cu-Ce) intermetallic phases at the interface between the eutectic Si and α-Al matrix. The chemical analysis by EDS studies of the Al-18%Si-3.6Cu-0.3%Ce alloy showed (Table 3) the presence of a Ce-rich phase

in the sidewall of the θ phase, which could be described as Al_2Ce-Si-Cu (Spectrum no-2). It can be clearly seen that Al_2Cu contains higher Ce (the mass fraction of Ce is approximately 16.79%) and Al_2Cu becomes coarser when Ce is added to the Al-Si-Cu alloy. It can be speculated that the variation of morphology is caused by the partial dissolving of Ce in Al_2Cu. In the Ce-modified alloy, Al_2Cu eutectic was more compact, with much smaller surface area compared to the base alloy.

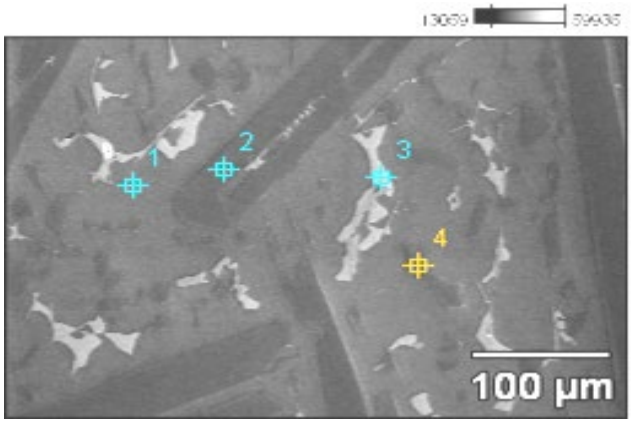

Figure 3. SEM/EDS micrograph of the cast Al-18%Si-3.6Cu alloy

Table 2. The composition analysis of different phases of by EDS

Spectrum position	*Phase*	*Al-K*	*Si-K*	*Fe-K*	*Cu-K*
pt1	α-Matrix	94.44	0.80	0.00	3.94
pt2	Primary Si	0.00	100.0	0.00	--
pt3	Al_2Cu	44.8	0.98	0.34	53.56
pt4	Eutectic Si	45.72	50.13	0.89	1.57

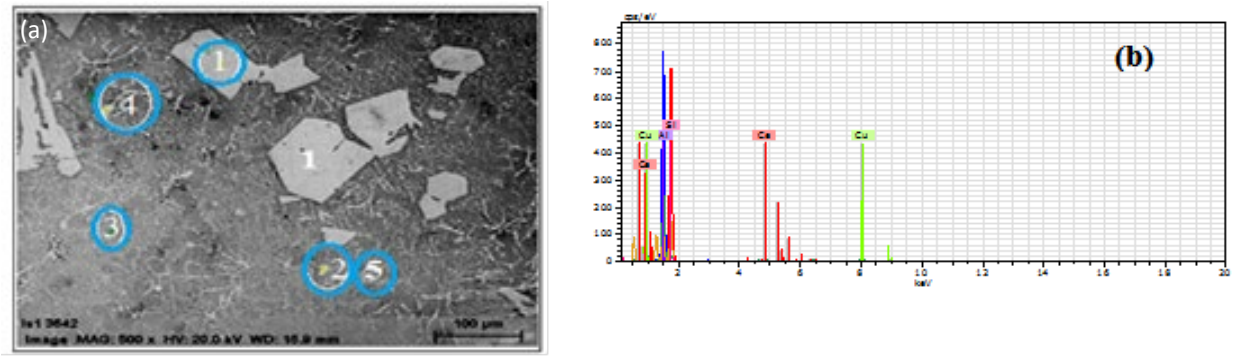

(a) **(b)**

Figure 4. SEM /EDS analysis of Ce modified Al-18%Si-3.6Cu alloy (b) EDS spectrum

Table 3. The EDS result of phase composition of Ce modified alloy

Spectrum position	*Phase*	*Al-K*	*Si-K*	*Fe-K*	*Cu-K*	*Ce-K*
pt1	Primary Si	0.94	98.90	0.00	0.16	0.00
pt2	Al_2Ce-Si-Cu	55.89	6.64	0.00	20.69	16.79
pt3	α-Matrix	98.09	0.97	0.34	0.91	0.02
pt4	Eutectic Si	32.91	65.00	0.89	1.94	0.15
Pt5	Al_2Cu	45.8	0.98	0.00	52.51	0.34

The SEM microstructures of the modified alloy after hardening for the 1hr, 3hr, 5 hr and7hr are shown in Figure 5. The microstructure of 1hr age hardened (Figure 5a) alloy depicts the presence of the primary Si and Si eutectic phases with rounded and fine precipitation of θ and Ce rich phases. The microstructure the modified and 5 hr age hardening (Figure 5c) alloy exhibited a significant volume fraction of medium-sized Al_2Cu intermetallic particles in the α-Al matrix. It can be seen by comparing Figure 5(b) and Figure 5(c) that the amount of fine Al_2Cu precipitates increased as the ageing period increases. However, the microstructure of the 7-hour aged alloy (Figure 5d) revealed the presence a coarse θ phase close to the Si phase. The increasing ageing time, the solute atoms segregate from the supersaturated solid solution and become fine θ precipitates initially and causing agglomeration of the precipitating phase form a coarse θ phase. The precipitation sequence in the Al-Si-Cu alloy is influenced by the high density of dislocations that form during quenching close to the Si-rich zone because of the high difference in thermal expansion between the Si particles and the α-Al matrix. As a result, the coarse phase develops on the dislocations close to the Si particles.

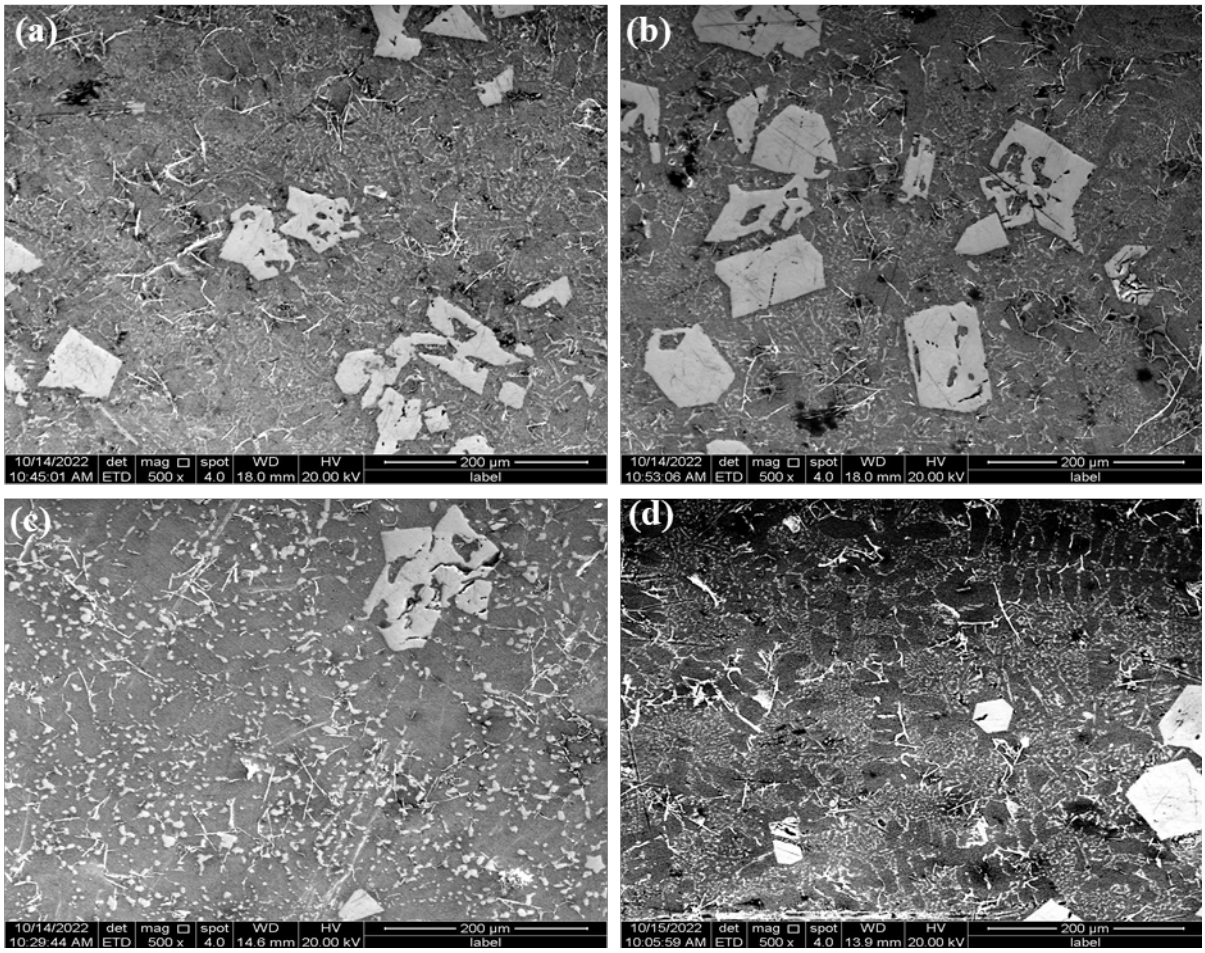

Figure 5. SEM microstructures of the modified and age hardening alloys after: (a) 1 hr, (b) 3hr, (c) 5hr and (d) 7hr

The cast Al alloys contain pro-eutectic solution, eutectic mixtures of Al and Si and precipitated particles. The solubility of Cu in the Al matrix increased owing to the high-temperature solution heat treatment. The dissolved solutes remain in the solid solution during quenching at room temperature. The microstructural evolution due to the aging treatment was mainly attributed to the increased precipitation of θ phase. Metastable precipitates with various structures sequentially appear and disappear as the alloys are aged. The precipitation pattern of diluted Al-Cu alloys is a well-known example represented as SSS → GP1 → GP2 (or θ″) → θ′ → θ. Where SSS is the supersaturated solid solution after solution treatment and quenching. Nano-sized coherent pre-precipitates (or solute clusters), called Guinier–Preston (GP) zones are formed during natural aging and in the early stages of artificial aging. Here, GP1 and GP2 refer to the solute-rich regions formed in the first and second stages of aging, whereas the θ′ and θ are stable

phases characterized by coarse and fine particles that are typically observed in over aged and optimum ageing conditions respectively [29]. At room temperature, Cu in the Al-Si alloy leads to the formation of GP zones and with a further increase in the temperature to 100°C leads to the dissolution of GP zones, forming a coherent θ' phase with a double-layer structure consisting of Al and Cu. Prolonged aging dissolves the GP zone and in homogeneously nucleates metastable phases on dislocations. Owing to the difference in thermal expansion coefficients of the primary Al and Si particles, low-energy and high-density dislocations form in Al-Si-Cu alloys. These sites act as heterogeneous nucleation sites for the θ' phase, forming a stable, incoherent (θ)-Al_2Cu phase) with aging, which increases the nucleation rate of the θ-Al_2Cu phase, suppressing the growth of Al_2Cu phase during aging, thereby increasing the volume fraction of the θ phase [30]. The fragmentations of Al, Al_2Cu, and Si eutectic phases within the matrix are redistributed during age-hardening. During the holding period, the dissolution of the Cu-rich phase raises the concentration of Cu and Si in the matrix. Finally, prolonged ageing causes precipitated particles to become coarse and incoherent with the Al matrix.

3.2. Hardness

Figure 6 shows the results of hardness values of the base, modified and age-hardened alloys. The hardness of the alloys with and without the Ce addition are 90 and 96 HB. The results indicated that the Ce addition contributed to an improved hardness value than the base alloy, possibly due to an increase in the fiber form of the eutectic Si phase. Furthermore, the age hardening treatment increased the hardness and the 5hr age hardened alloy showed the highest hardness of 125 HB. However, with a further increase in the ageing time, the 7hr age hardened alloy showed a lower hardness value of 114 HB. The increase in hardness in the modified alloy could be owing to the formation of nearly spherical primary Si and changed dendrite eutectic silicon into a fine fibrous form and relatively hard Al_2Cu and Al_2CeSi phases in the refined Al matrix. Higher hardness may be partially attributed to Ce dissolving in Al_2Cu. The presence of the Ce-rich phase close to the Al_2Cu phase increased the hardness. The solid solubility of Cu in Al-matrix during the solution treating process could also be attributed to an increase in the hardness of the alloy. The precipitates of fine particles Al_2Cu in the matrix and spherical eutectic Si phases obtained during the age hardening reduced the stress concentration at the interface of Si particles and α-Al matrix. As a result, the tendency to initiate subsurface cracks decreased, resulting in an increase in hardness. With increasing ageing time, the solute atoms segregate from the super saturated

solid solution and become fine Al_2Cu precipitates initially and gradually become coarse and incoherent with the matrix. This makes it easy for the dislocations to penetrate the surface and lowers the shear stress and thus, decreases the hardness [31].

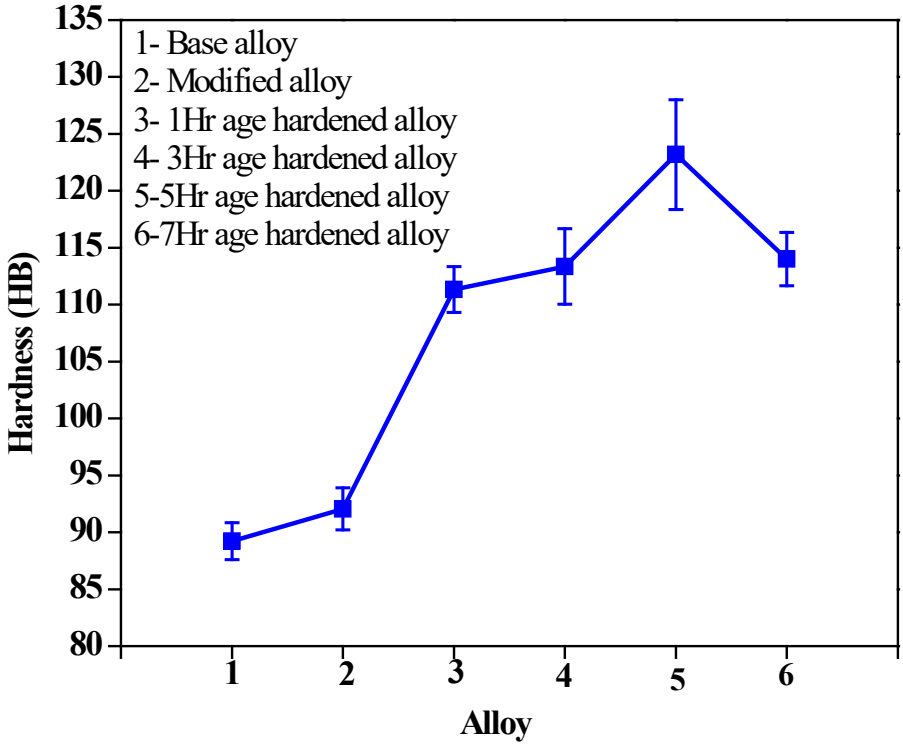

Figure 6. Hardness of base, modified and modified with heat treated alloys

3.3. Interface temperature

The variation of interface temperature with the load is shown in Figure7 at a constant sliding speed of 1.0 m/s. It is observed that the interface surface temperature increases linearly with the increasing load. The base alloy shows a higher interface temperature than that in the modified and heat-treated conditions. The alloys in age hardening condition do not affect the interface temperature substantially; however, the interface surface temperature decreases with the increasing age hardening time. It is observed that the 5hr age-hardened alloy exhibits low interface surface temperature throughout the load range compared to the other age hardened alloys. The amount of oxidation formation and thermal softening of the matrix depends on the interface temperature, which influences the wear rate and friction force. The presence of coarse primary Si particles with sharp edges and corners, needle-like eutectic phase and brittle intermetallic phases in the base alloy are less cohesive with the matrix, which causes the matrix to soften easily and the high plastic flow of metal. This results in increasing the area of contact,

leading to a high friction force and a high interface temperature. The cast condition, Si and intermetallic phases of the alloy act independently that may facilitate the yielding of asperities and increasing the actual area of contact, hence, increase in the interface temperature. The modified and heat-treated alloy has a high hardness and strength due to the modified Si particles, fine precipitation of Al_2Cu intermetallic, increased solid solubility, and greater cohesiveness with the matrix, which resists asperity yielding and gross plastic deformation near the surface layer, making the oxide protective film more stable and reducing the real area of contact resulting in less interface temperature [32].

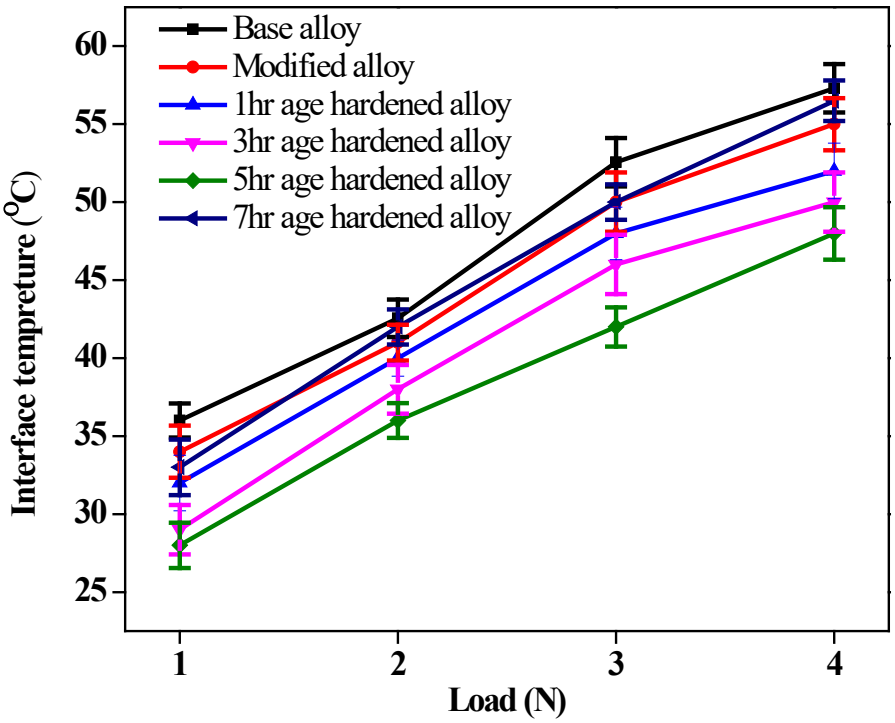

Figure 7. The variation of the interface temperatures with the load at a sliding velocity of 1.0m/s

3.4. Wear behavior

Figure 8 depicts the variation in wear rates with loads at sliding velocity of 1.0 m/s. It has been noted that the wear rate increases as load increases, and as expected, the base alloy exhibits a higher wear rate than the modified alloy. The age-hardened modified alloys show a lower wear rate and 5 hr age hardened alloy exhibits the least wear rate as compared to the 1hr, 3hr and 7 hr age-hardened alloys. At the loads of 10, 20, 30, and 40 N, the 7hr age-hardened alloy exhibits approximately 17%, 57%, 70%, and 67%, higher wear rates respectively compared to the 5hr age

hardened sample. Figure 9 depicts the relationship between the load and wear resistance (reciprocal of wear rate) of the basic, modified, and age hardened alloys. It has been found that the wear resistance diminishes with the increasing load and is greater at a low load of 10 N. The base alloy has lower wear resistance than the modified alloy, and as the age hardening time increases, the wear resistance rises. The 5hr age-hardened alloy, in contrast, shows the highest wear resistance over the entire load range, while the 7hr age-hardened alloy exhibits lower wear resistance.

Age hardening also increases the hardness due to increased area fraction of clusters of Al_2Cu phase along the interface of primary Si particles. The diffusion of the alloy increases the bonding between Si and the Al-matrix resulting in a higher resistance of the matrix to plastic flow [33]. Uniform distribution of fine and spheroidized Si crystals surrounded by fine precipitates of Al_2Cu would retard the nucleation and crack propagation and therefore, can be attributed to the high wear resistance of the 5hr age hardening alloy. As the aging time (7hr) increased, hardness decreased because the precipitates transformed gradually from metastable state to a stable state, and finally to an incoherent interface between the precipitates and matrix. According to Ostwald ripening [30], the solute atoms get segregated from the supersaturated solid solution and coarsening of precipitates by dissolution of the smaller precipitations due to reduction of surface energy. When the precipitates become large and few, the distance between the precipitates increases, therefore surface becomes easier for the dislocations to pass through and resulting in a decrease in shear stress and therefore decrease in the hardness and wear resistance.

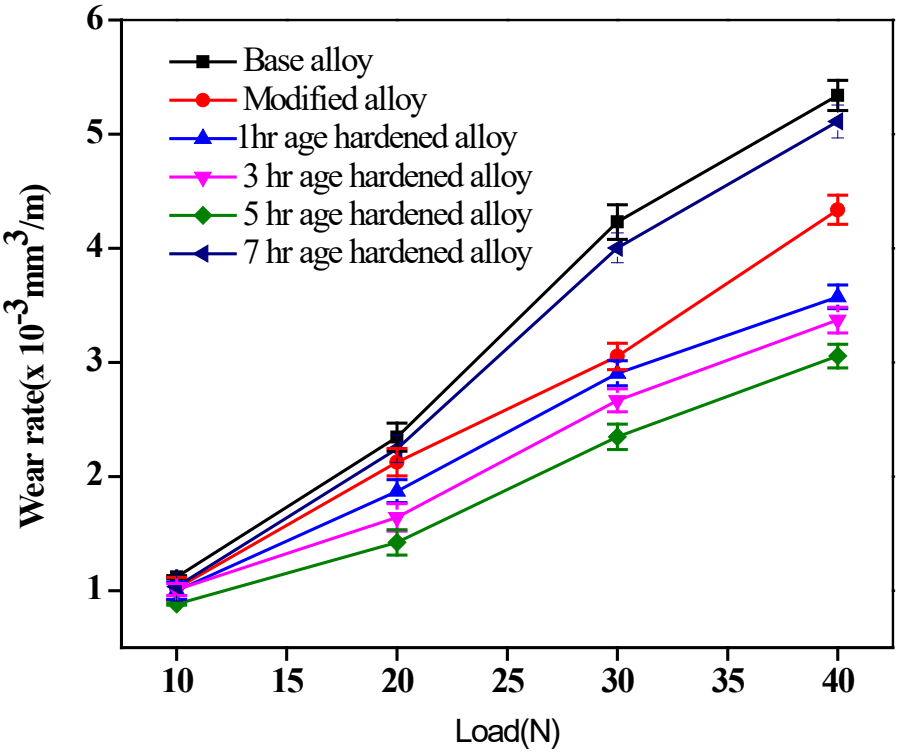

Figure 8. The variation of wear rates with the loads at 1.0 m/s sliding velocity

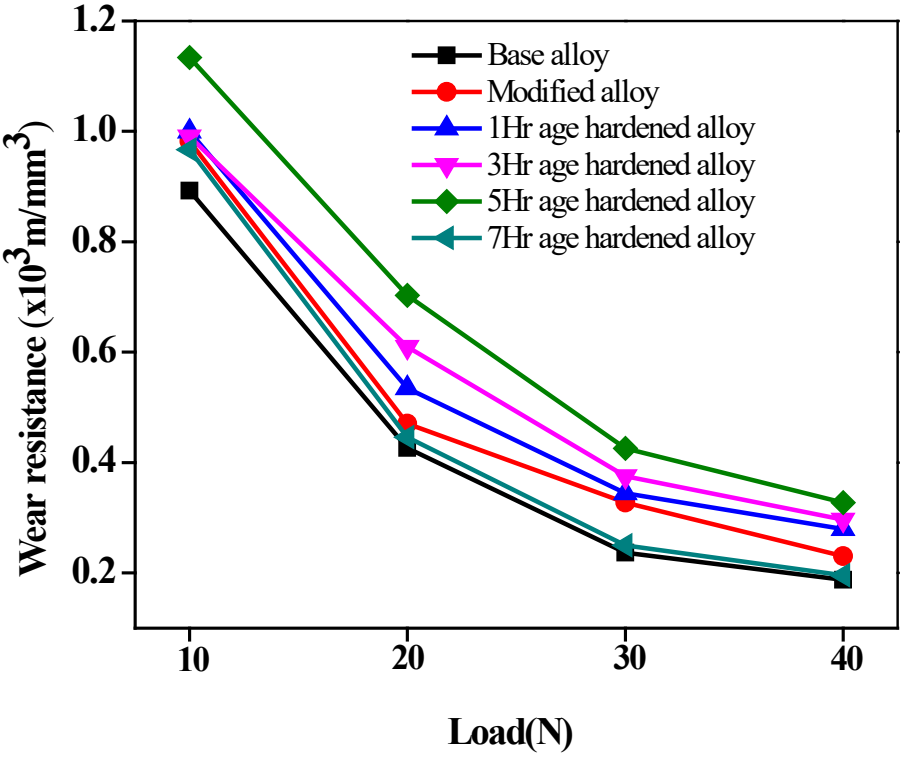

Figure 9. Variation of wear resistance with the load at 1.0m/s sliding velocity.

The specific wear rates of the base, modified and aged alloys under different loads are shown in Figure10. In the present investigation, it was observed that the specific wear rate varied in a range between 10^{-04} to 10^{-03} mm^3/N-m. According to the values of the specific wear rates, the state of wear was classified as mild wear (w_s=10^{-07} to 10^{-04} mm^3/N-m) caused by oxidative wear and severe wear ($w_s \geq 10^{-03}$ mm^3/N-m) induced by adhesive and abrasive wear [34].

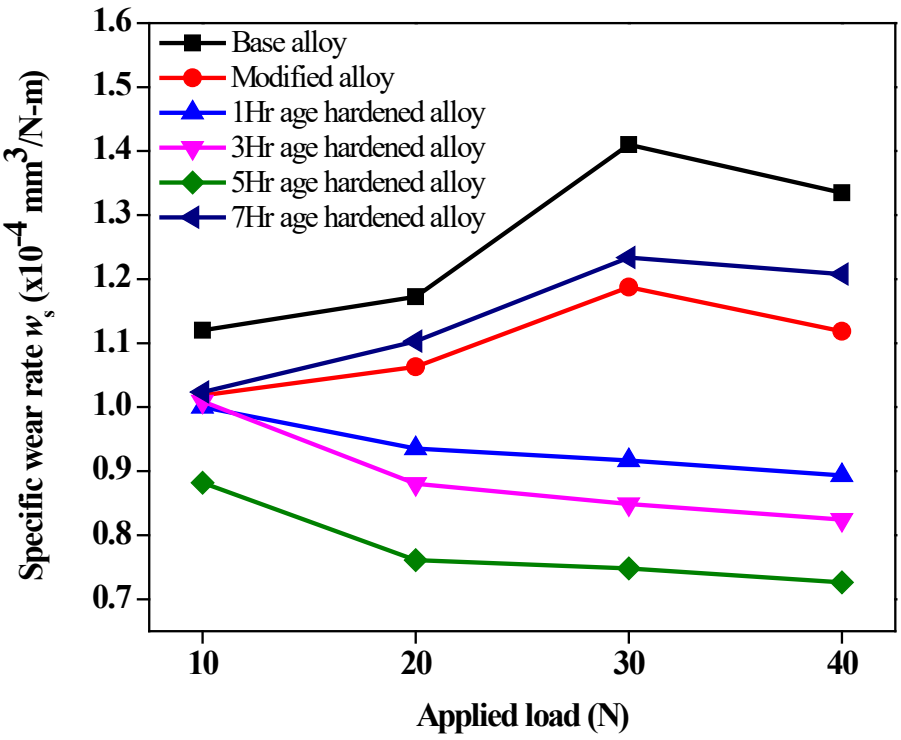

Figure 10. The variation of the specific wear rates with the load and sliding velocity of 1.0 m/s

It has been shown that the specific wear rate for basic alloys, modified alloys, and 7-hour aged alloys increases in the low load range between 10N and 30N and further decreases at high loads between 30N and 40N. The specific wear rates of the other age hardened alloys gradually decreased with the aging times and the 5 hr age hardened alloy showed a low specific wear rate. An increase in load results in an increased real contact area between the mating surfaces, which gives rise to an increased wear rate. The high wear rate in the base alloy was attributed to the penetration of the hard and coarse primary Si particles in the matrix. The modified alloy showed a reduced wear rate owing to the presence of smooth edges, near-spherical morphology of Si and eutectic silicon phases and refined grains of Al matrix. This would cause low stress concentration at the particle-matrix interfaces and resist the crack nucleation and their growth. Furthermore, the precipitation of fine intermetallic Al_2Cu phase distributed in the inter-dendritic

regions may be attributed to the reduction in the wear rate [35]. The Al_2Cu precipitates at the grain boundaries of the primary Si phase strongly strengthen the matrix during ageing by increasing the bonding between the spherical Si, the second phase particles, and the matrix, resulting in greater resistance to plastic flow [36]. On the other hand, increased ageing time increases the diffusion rate and precipitation of high volume of the hard Al_2Cu phase, resulting in an increase in hardness [37]. The presence of near-spherical morphology of hard primary Si and eutectic silicon phases, Al_2Cu and Al_2CeSi intermetallic phases in the soft Al matrix can enhance hardness and give better wear resistance. The strengthening of alloys by the formation of fine precipitates that is highly coherent with the matrix. Once the coarsening of the precipitates occurs, they cannot be coherent with the matrix again. Kaçar et al. [38] indicated that in the over-aged (7 hr) condition, the precipitates were relatively large, and this significantly reduced the hardness and wear resistance.

3.5. Co-efficient of friction (μ)

The variation of the average coefficient of friction with the load is shown in Figure 11. The coefficient of friction was found to be low at 10N and increased with increasing the load. The μ values of the modified alloy had a lower coefficient of friction than the base alloy, and the age hardened alloy revealed a lower coefficient of friction and a declining trend with increasing aging time. In addition, it was observed that the 5hr aged alloy had the lowest coefficient of friction compared to the other alloys. The alloy aged for 5h causes spheroidization of Si phase and increases the volume fraction of hard Al_2Cu particles. These changes in the microstructure of 5 hr age-hardened alloy relieve the stress concentration at the interface of the Si/Al and therefore, can effectively suppress crack propagation at the spheroidized Si and Al interface. Thus, reducing fracture and deformation of the surface asperities results in a low coefficient of friction. This reduction in the coefficient of friction may attribute to the fact that higher amount of precipitates and higher hardness of the aged alloys may reduce the real contact area.

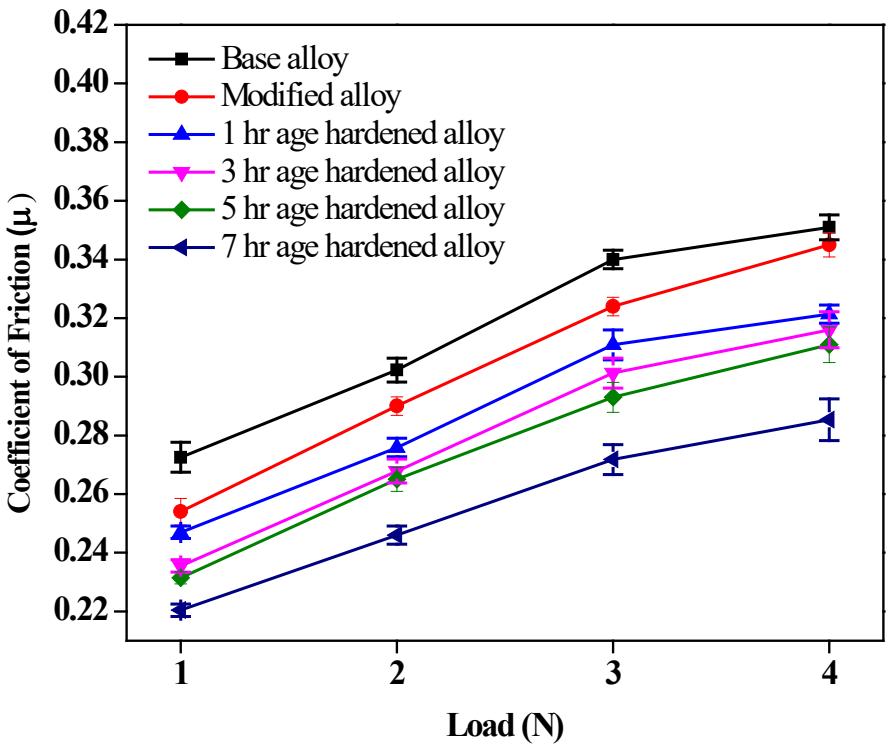

Figure 11. The variation of the average coefficient of friction with the load at a sliding velocity of 1.0 m/s

3.6. Worn surface morphology and wear map

Figure12 displays the worn surfaces of the base, modified, and age-hardened alloys after sliding for 2000 m at 40 N load and 1.0 m/s sliding velocity. It was observed in the worn surface of the base alloy (Figure 12a) exhibited marks of severe damage, the higher degree of deep grooves, scratches, furrows, and the delamination surface with large cavities. Cracks in the vertical direction of the wear track, and spalling on both sides of the wear track, indicated adhesive wear. At a higher load of 40 N, the softening of the surface took place due to the frictional resistance resulting from the surface material of the alloy getting welded to the counter face surface. Due to the increase in adhesive nature of the pin and the alloy, delamination occurs easily. The worn surface of the modified alloy is shown in Figure12(b). It was observed that the extent of delamination appeared to be less compared to that of the base alloy. The depth of valleys and the width of grooves were found notably less, and the undulations observed on the worn surface were considerably less. Figure 12(c-e) depicted the worn surface of modified and age-hardened alloys. As a result of mild wear, it had a reasonably smooth surface with fine abrasion grooves. The worn surface also had a tiny number of small dimples and only a few scoring marks

stretching from one end to the other. The worn surface of the modified 5 hr age hardened alloy (Figure 12d) revealed a smooth surface, with fine scoring and uniform wide grooves. It is also observed that white areas on the surface are indicative of oxide formation.

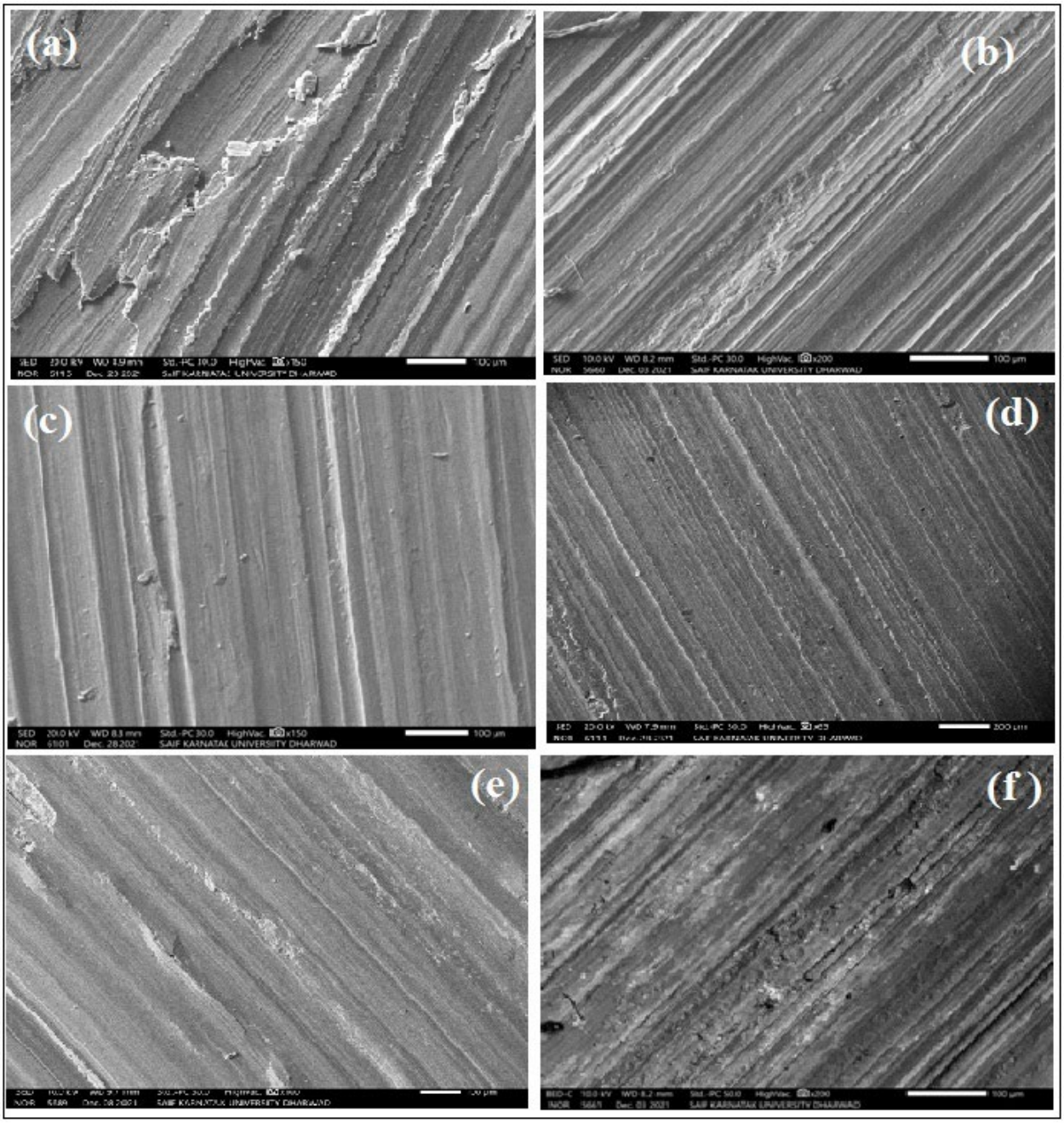

Figure 12. SEM worn surfaces at the load of 40N and sliding velocity of 1.0 m/s for(a) base (b) modified, (c) 1hr aged, (d) 3hr aged, (e) 5hr aged and (f) 7hr aged alloys.

Figure 13 shows different wear regimes as a function of the loads. The wear map was constructed based on wear rate values and the worn-out surface morphologies. Low to moderate wear was controlled by oxidation wear, while mild wear was primarily controlled by oxidation and the abrasive mode of wear. Severe wear was prominently controlled by plastic deformation (adhesive wear) and abrasive wear. It was observed from the figure that the base alloy showed mild wear at loads up to 30 N and beyond, and the wear mechanisms of the base alloy could be defined by both oxidative and abrasive wear. At a higher load closer to 40 N, the wear in the base alloy was severe (plastic deformation induced), and the wear mechanism was controlled by both adhesive and abrasive mechanisms. In the modified alloy, up to a load just beyond 10 N, there existed low mild wear (purely oxidative), a larger mild wear regime, and a transition from mild wear to severe wear closer to 40N load. The severe wear regime was smaller in the modified alloy as compared to the base alloy. This could be due to the modification of Si, eutectic Si, and intermetallic phases. A comparison of wear among the age-hardened alloys showed the largest severe wear regime in the 7-hr age-hardened alloy, whereas the 5 hr age-hardened alloy showed very minimal severe wear. Because of the high hardness and abundance of small Al_2Cu precipitates, alloys that have been age-hardened for five hours may not experience as much severe wear. At higher load, the wear mode combines a little oxidative, more adhesive, and abrasive forces. However, the Ce-modified alloy with 5-hr age hardening produced the best wear behavior at all loads between 10 and 40 N.

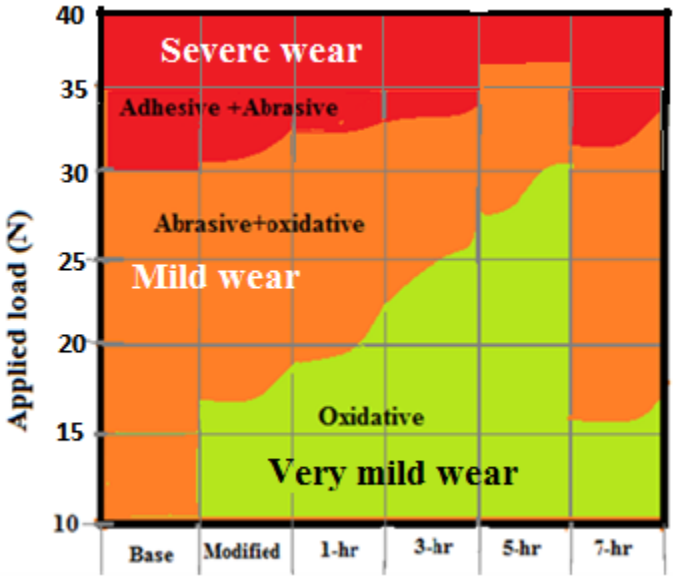

Figure13. The wear mechanism map at different loads and 1.0 m/s sliding velocity.

4. Conclusion

The effects of microstructural modification by Ce addition and post-heat treatment by age hardening at various ageing periods on the wear properties of an Al-15Si-3.6Cu alloy were investigated and the following conclusions can be drawn.

1. The cerium modified alloy microstructure demonstrated a significant change in the primary Si coarse sharp edges, long needle/acicular eutectic phases, and intermetallic phases into spherical and globular eutectic Si and intermetallic particles. The microstructure of the modified and age hardened alloy revealed precipitation of fine Al_2Cu and further refining of eutectic Si and Al-Si-Ce phases.

2. Increasing ageing time increased the amount of precipitated particle at the grain boundary, which hindered the dislocation movement. With the further increase in the ageing time, the precipitated participles became coarse and incoherent with the matrix. The coarse particles allowed the dislocations to move freely.

3. The hardness of the modified alloy was higher than the base alloy. The modified and age hardened alloy reached the maximum hardness at 5 hr age hardening condition.

4. The wear properties of Al-15Si-3.6Cu alloy are considerably improved by the addition of the Ce modifier and age hardening. The wear rates of modified and age-hardened alloys increased with an increase in the ageing time and the 5 hr age-hardened alloy showed the lowest wear under the loads ranging from 10 to 40N.

5. The interfacial temperature and friction coefficient of the modified and age-hardened alloys were less than the base alloy. The 5 hr age-hardened alloy exhibited the lowest coefficient of friction in the entire load range, which indicated a higher wear resistance.

6. All modified and age-hardened alloys showed a transition from lower mild to mild and to severe wear mechanisms but the 5hr age-hardened alloy displayed very little sever wear and smallest mild wear zones for the selected loading conditions.

Acknowledgement

The authors would like to thank the Mechanical Department of Tontadarya College of Engineering, Gadag, for providing the necessary facilities and the support for this work.

References

[1] Dayanand M. Goudar, Veeresh T. Magalad, Rajashekar V. Kurahatti (2020): Study of microstructure and tribological behavior of spray cast high silicon hypereutectic Al-Si alloy, Advances in Materials and Processing Technologies, DOI: 10.1080/2374068X.2020.1855402.

[2] V, V., Narayan Prabhu, K. Review of Microstructure Evolution in Hypereutectic Al–Si Alloys and its Effect on Wear Properties. *Trans Indian Inst Met***67**, 1–18 (2014). https://doi.org/10.1007/s12666-013-0327-x

[3] J.H. Abboud and M. Kayitmazat. Microstructural evolution and hardness of rapidly solidified hypereutectic Al-Si surface layers by laser remelting. advances in Materials and ProcessingTechnologies,2022,89(4),4136–4155 https://doi.org/10.1080/2374068X.2022.2037352

[4] Jaafar Hadi Abbouda and Jyoti Mazumder. Ultra-refined primary and eutectic silicon in rapidly solidified laser produced hypereutectic Al–Si alloys. Advances in, Materials and ProcessingTechnologies,2022,8(3)2510–2532.https://doi.org/10.1080/2374068X.2021.1913326

[5] M. Elmadagli, T. Perry, A.T. Alpas, A parametric study of the relationship between microstructure and wear resistance of Al–Si alloys, Wear. Volume, 4

[6] Hanshan Dong, Surface Engineering of Light Alloys. Aluminium, Magnesium and Titanium Alloys A volume in Wood head Publishing Series in Metals and Surface Engineering, Book**,** 2010.

[7] Ren-Guo Guan, Di Tie. A Review on Grain Refinement of Aluminum Alloys: Progresses, Challenges and Prospects. Acta Metallurgica Sinica (English Letters) 2017 , 30 (5): 409-432 https://doi.org/10.1007/s40195-017-0565-8.

[8] Kazuhiro Nogita, Stuart D. McDonald, Arne K. Dahle. Eutectic Modification of Al-Si Alloys with Rare Earth Metals. Materials transactions Volume 45 (2004) Issue 2 323- 326. https://doi.org/10.2320/matertrans.45.323.

[9] R. Ahmada, Z. M. Sheggafa, M. B. A. Asmaelb and M. Z. Hamzah. Effect of rare earth addition on solidification characteristics and microstructure of ZRE1 magnesium cast alloy. Advances in Materials and Processing technologies, 2017vol.3,no.3,418–427https://doi.org/10.1080/2374068X.2017.1336687

[10] Omid Mehrpour,Mostafa Jafarzadeh ,Mohammad Abdollahi, A Systematic Review of Aluminium Phosphide Poisoning. Archives of Industrial Hygiene and Toxicology. Vol 63(1) 2012) Page 61 - 73. DOI: https://doi.org/10.2478/10004-1254-63-2012-2182

[11] Juan Asensio-LozanoBeatriz Suàrez. Effect of the addition of refiners and/or modifiers on the microstructure of die cast Al–12Si alloys. 2006.Scripta Materialia 54(5):943-947. DOI:10.1016/j.scriptamat.2005.10.067

[12] Henghua ZHANG, HailiDUAN, GuangjieSHAO, LuopingXU, JunlinYIN BiaoYAN. Modification mechanism of cerium on the Al-18Si alloy. Rare. 2006, Pages 11-15.https://doi.org/10.1016/S1001-0521(06)60006-5.

[13] QinglinLi,TiandongXia,YefengLan,WenjunZhao,LuFan[a]PengfeiLi. Effect of rare earth cerium addition on the microstructure and tensile properties of hypereutectic Al–20%Si alloy, Compounds Vol, 15, 2013, Pages 25-32

[14] Stanislav Kores, Maja Vonina, Borut Kosec, Primo` Mrvar, Jo`ef Medved, Effect of cerium additions on the alsi17casting alloy. MTAEC9, 44(3)137(2010), UDK 669.131:669.85/.86.

[15] J. Gröbner, D. Mirković, and R. Schmid-Fetzer, Metallurgical and materials transactions A, Volume 35A, November (2004) 3349.

[16] Hosseinifar, Mehdi, Malakhov, Dmitri V, Physical Metallurgy and Thermodynamics of Aluminum Alloys Containing Cerium and Lanthanum July 2009 http://hdl.handle.net/11375/17315

[17] Xiao-hui Ao, Shu-ming Xing,Bai-shui Yu ,Qing-you Han. Effect of Ce addition on microstructures and mechanical properties of A380 aluminum alloy prepared by squeeze-casting. International Journal of Minerals, Metallurgy, and Materials volume 25, 2018 pages 553–564.

[18] Williams S. Ebhota and Tien-Chien Jen. Intermetallics Formation and Their Effect on Mechanical Properties of Al-Si-X Alloys.Doi10.5772/intechopen.68256.ISBN978-1-78923-179-3 Print ISBN978-1-78923-178-6,eBook (PDF) ISBN978-1-83881-298-0,DOI: 10.5772/intechopen.73188

[19] Yan Zheng, Wenlong Xiao, Sujing Ge, Weitao Zhao, Shuji Hanada, Chaoli Ma. Effects of Cu content and Cu/Mg ratio on the microstructure and mechanical properties of Al–Si–Cu–Mg alloys.CompoundsVolume 649, 15 November 2015, Pages 291-296

[20] Lorella Ceschini , Stefania Toschi ,Friction and Wear of Aluminum Alloys and Composites,2017, Doi: https://doi.org/10.31399/asm.hb.v18.a0006388.

[21] R. Dasgupta, S.K. Bose. Effect of Copper on the tribological properties of Al-Si alloys. J. of Material sc. Letters, 14 (1995), pp. 1661-1663.

[22] Shivaprasad Channappagoudar a, Kiran Aithal, Narendranath Sannayallappa Vijay Desai , Pudukottah Gopaliengar Mukunda.The Influence of the Addition of 4.5 wt.% of Copper on Wear Properties of Al-12Si Eutectic Alloy. Jordan Journal of Mechanical and Industrial Engineering,9 (3),.2015, 217 - 22

[23] K. G. Basava kumar, Mukunda Pudukottah, P.G. Mukunda, M. Chakraborty, Dry sliding wear behavior of Al–12Si and Al–12Si–3Cu cast alloys. Materials & Design, 30, 4, l 2009, Pages 1258-1267.

[24] Emma Sjölander, Salem Seifeddine. The heat treatment of Al–Si–Cu–Mg casting alloys. Journal of Materials Processing Technology210, 10, 2010, 1249-1259

[25] Arne Wahlen,H. Lüchinger, Peter J. Uggowitzer. On the silicon spheroidization in Al-Si alloys Journal of Light Metals, 2002,2(4):263-269,DOI:10.1016/S1471-5317(03)00010-5

[26] Biplab Hazra, Supriya Bera,Bijay Kumar Show. High temperature wear micro mechanisms in Al–17Si–5Cu alloy after an isothermal heat treatment. Materials Corrosion and Degradation, 2021, 60(3),https://doi.org/10.1080/00084433.2021.1997264

[27] R. Ahmad & M.B.A. Asmael. Influence of Cerium on Microstructure and Solidification of Eutectic Al-Si Piston Alloy, Materials and Manufacturing Processes, DOI:10.1080/10426914.2015.1127942

[28] Maja VONČINA, Jožef MEDVED, Tonica BONČINA, Franc ZUPANIČ. Effect of Ce on morphology of α(Al)−Al_2Cu eutectic in Al−Si−Cu alloy, Trans. Nonferrous Met. Soc. China 24(2014) 36−41.

[29] Hiroshi Miyoshi , Hajime Kimizuka, Akio Ishii, Shigenobu Ogata. Competing nucleation of single and double-layer Guinier–Preston zones in Al–Cu alloys, Scientific Reports, 2021 11:4503https://doi.org/10.1038/s41598-021-83920-8

[30] A.M.A. Mohamed and F.H. Samuel, Review on the Heat Treatment of Al-Si-Cu/Mg Casting Alloys. http://dx.doi.org/10.5772/79832.

[31] Muddle, B.C. and Polmear, I. J., The precipitate phase in Al-Cu-Mg-Ag alloys. Acta Metallurgica Material, 1989, 37, p. 777.

[32] Xu. C L, Yang. Y F,et al . Effects of modification and heat-treatment on the abrasive wear behavior of hypereutectic Al–Si alloys. J. Mater. Sci. 2008;. 42:6331-6338

[33] Expressing Wear Rate in Sliding Contacts Based on Dissipated Energy. Huq, M.,Z., Celis, Jean-Pierre. Wear, 2002, 252.

[34] Erika F. Prados , Vitor L. Sordi, Maurizio Ferrante,The effect of Al2Cu precipitates on the microstructural evolution, tensile strength, ductility and work-hardening behaviour of a Al–4 wt.% Cu alloy processed by equal-channel angular pressing. Acta Materialia,2013,6(1),115-125.

[35] A.S.Anasyida, A.R.Daud,M.J.Ghazali.Dry sliding wear behavior of Al–12Si–4Mg alloy with cerium addition. Design. Vol,2010, Pages 365-374

[36] Xu. C L, Yang. Y F,et al . Effects of modification and heat-treatment on the abrasive wear behavior of hypereutectic Al–Si alloys. J. Mater. Sci. 2008; 42:6331-6338

[37] Prasad.B.K, Dan.T K. Influence of solutionzing temperature and duration on the microstructure and properties of a hypereutectic aluminum-silicon alloy-graphite composite. J. Mater. Sci. Letts.1991;10:1412-1414

[38] Hülya Kaçar, Enver Atik, Cevdet Meriç.. The effect of precipitation-hardening conditions on wear behaviors at 2024 aluminum wrought alloy. J. Materal. process. Tchnol.2003;142:762-766.